Vol. 03, Iss. 3 (2025) 340-349, DOI: 10.61552/JME.2025.03.009

JME

Journal of Materials and Engineering

www.jme.aspur.rs

Research article

Influence of Fiber Content on Microstructure and Surface Performance of Abaca Fiber Reinforced Epoxy Composites

Dragan Dzunic[a,*], Marko Milosevic[b], Zivana Jovanovic Pesic[a], Vladimir Kocovic, Suzana Petrovic Savic[a], Aleksandar Djordjevic[a], Slobodan Mitrovic[a]

[a]*University of Kragujevac, Faculty of Engineering, Kragujevac, Republic of Serbia,*
[b]*The Academy of Applied Studies Polytechnic, Belgrade, Serbia.*

Keywords:

Abaca fiber
Epoxy composite
Fiber content
Tribological behaviour
Wear resistance
Vacuum infusion

* Corresponding author:

Dragan Dzunic
E-mail: dzuna@kg.ac.rs

Received: 12 September 2024
Revised: 24 October 2024
Accepted: 11 November 2024

A B S T R A C T

This study examines the tribological behaviour of epoxy composites reinforced with abaca fibers, with particular attention to the influence of fiber content on surface response under sliding conditions. Composite specimens containing 10%, 20%, and 30% fibers were produced using vacuum infusion to ensure controlled impregnation and uniform reinforcement distribution. The samples were tested under dry sliding conditions using a CSM nanotribometer in a ball-on-plate configuration with a contact radius of 2 mm, a normal load of 300 mN, a sliding speed of 10 mm/s, and 500 cycles.

Composites with lower fiber content exhibited lower coefficients of friction and smaller penetration depths. These lower friction values correlate with the higher matrix continuity observed in optical micrographs. Increasing fiber content led to a higher density of structural imperfections, including voids, which reduced friction stability and influenced wear behaviour. Optical microscopy revealed air bubbles within the surface layer and differences in wear debris distribution depending on fiber fraction.

Under the applied low-load conditions, tribological performance was governed primarily by fiber distribution quality and processing-induced defects rather than fiber content alone.

© 2025 Journal of Materials and Engineering

1. INTRODUCTION

In mechanical systems operating under sliding contact, material degradation and friction directly influence maintenance intervals and operational costs. Friction losses account for a considerable share of global energy use, while excessive wear often results in premature component failure, unexpected downtime, and higher life cycle costs. For these reasons, improving tribological performance is both a technical necessity and an important economic objective.

In industrial applications involving sliding contacts, improved tribological performance contributes to longer service intervals and reduced downtime. The contact response depends on material properties, surface condition, applied load and operating environment. Careful tribological design can significantly enhance reliability, extend service life, and reduce both energy losses and maintenance demands.

Tribological properties of materials, coatings, and lubricants are typically evaluated using parameters that describe friction and wear behaviour. These include the coefficient of friction in the contact zone and indicators of material degradation such as wear volume, wear rate, and surface damage characteristics. A meaningful assessment therefore requires not only measurement of these parameters, but also an understanding of the mechanisms governing surface interaction and lubrication under boundary, mixed, and hydrodynamic conditions.

Holmberg and Erdemir [1] presented a thorough analysis indicating that about 23% of global energy consumption, approximately 119 exajoules (EJ) annually, is related in some way to friction and wear in mechanical systems. Their results put into perspective how significant tribological losses are across sectors such as industry, transportation, and power generation, where large numbers of components operate under continuous sliding or rolling contact.

Their estimates suggest that roughly 103 EJ, close to 20% of total global energy use, is spent simply on overcoming friction between contacting surfaces. An additional 16 EJ, or about 3%, is associated with the consequences of wear. This includes the energy needed to manufacture replacement parts as well as the costs related to maintenance activities and production downtime. When viewed at the global scale, these figures make it clear that even modest improvements in friction reduction or wear resistance could lead to substantial energy and material savings.

Building on these findings, improvements in materials and tribological design have the potential to reduce energy losses in a meaningful way. Estimates suggest that a substantial portion of industrial energy consumption is associated with overcoming friction in a wide range of mechanical systems. In transportation applications, where components operate continuously under contact loading, this share can be even higher.

Reducing friction in such systems therefore has direct implications for overall energy efficiency. Within a single production facility, thousands of contact interfaces operate simultaneously, each contributing to cumulative energy losses. While material wear cannot be entirely avoided, its progression can be limited through appropriate material selection, surface engineering, and the application of well-designed lubrication strategies.

Friction and the associated energy losses can be reduced through appropriate engineering measures. Material selection and surface processing of contact elements are key parameters in friction control. Surface integrity and compatibility between contacting materials play a decisive role in determining friction behaviour.

Additional improvements can be achieved through surface engineering solutions, including advanced coatings, nanostructured layers, and chemical or physico-chemical treatments that modify surface hardness, roughness, and adhesion characteristics.

The demand for products with longer service life, lower weight, and reduced manufacturing costs has encouraged the development of advanced engineering materials. Among these, composite materials have gained considerable attention, particularly those reinforced with natural fibers. Such composites offer a favorable balance of mechanical performance, low density, and environmental compatibility when compared to conventional base materials.

Although synthetic materials remain widely used in engineering applications, they are often associated with certain limitations, particularly in terms of production cost and environmental impact. Several studies have pointed out these concerns, including the work of Nägeli et al. [2], Dente et al. [3], and Shahinur and Hasan [4]. As a result, increasing attention has been directed toward the development of composite materials based on renewable resources.

Natural fibers have emerged as promising reinforcement materials due to their low density, availability, and reduced environmental footprint. Depending on their origin, they are generally classified as plant, animal, or mineral fibers [5–7]. Their incorporation into polymer matrices has opened new possibilities for producing materials that combine acceptable mechanical performance with improved sustainability.

The tribomechanical behaviour of plant fibers and the composites reinforced with them has a direct impact on the durability and service life of engineering components. The tribological response of such materials depends primarily on the characteristics of the matrix, the reinforcement, and the quality of the interfacial bonding between them [8–10]. The effectiveness of stress transfer across the interface, as well as the integrity of the composite structure, largely determines friction stability and wear resistance.

In addition to intrinsic material properties, operating conditions also play an important role. Parameters such as applied load, sliding speed, and environmental exposure can significantly influence the observed tribological performance [11, 12].

Composite materials have been the subject of continuous research for several decades, largely because of their potential to reduce material usage and improve energy efficiency in engineering systems. Lower friction levels contribute directly to reduced energy losses, while enhanced wear resistance extends component service life and decreases the need for frequent replacement.

Despite these advantages, achieving a uniform distribution of reinforcement within the matrix remains a significant challenge in composite manufacturing. In lightweight composite systems, where mass reduction is often a primary objective, the type of fiber, its dimensions, and its volume fraction strongly influence the overall mechanical and surface-related properties of the material. Careful control of these parameters is therefore essential to ensure consistent performance.

Liu et al. [13] investigated phenolic resin composites reinforced with 0–4 wt.% abaca fibers. Their results showed an improvement in wear resistance compared to the neat matrix, with the positive effect becoming more evident as the fiber content increased within the examined range. These findings suggest that even relatively small additions of natural fibers can influence surface durability under sliding conditions.

In the case of hybrid composites, several studies have reported that combining different types of fibers may lead to improved overall performance. For instance, epoxy composites reinforced with a mixture of jute and hemp fibers demonstrated higher wear resistance than systems containing only a single fiber type [14]. Such results indicate that hybrid reinforcement can modify the wear mechanism and improve load distribution within the composite structure.

Fiber orientation is another parameter that significantly affects the tribological response of natural fiber composites. Chin and Yousif [15] reported that positioning kenaf fibers perpendicular to the sliding direction increased wear resistance of an epoxy matrix by up to 85%. In their study, sliding speed and normal load had a comparatively smaller effect on the specific wear rate, whereas fiber orientation played a dominant role in shaping both friction behaviour and wear performance. Specimens with normally oriented fibers exhibited more stable and consistent behaviour than those with parallel or antiparallel alignment.

Comparable effects of fiber orientation were found in kenaf/epoxy composites tested under wet conditions. Fibers perpendicular to the sliding direction improved wear performance by roughly 35–57% over parallel or random alignments [16]. The authors explained this by better load transfer and less fiber pull-out, which slowed down surface damage.

In jute/epoxy composites, orientation also played a major role. Interestingly, the antiparallel configuration gave the best wear resistance, followed by parallel and then normal alignment [17]. This suggests that the ideal fiber direction may vary depending on fiber type, interface properties and matrix behaviour.

For abaca-based friction composites, alkali treatment strengthened fiber–matrix bonding and reduced wear under sliding [13]. Good adhesion at the interface clearly helped wear resistance at the right fiber loading. Overall, both fiber arrangement and interface quality need to be optimized for tribologically efficient natural fiber composites.

Based on these considerations, the present study focuses on evaluating the tribological behaviour of abaca fiber-reinforced epoxy composites with varying fiber content under controlled sliding conditions. The experimental procedure is described in the following section.

2. MATERIALS AND METHOD

Composite specimens based on epoxy resin reinforced with abaca fibers were fabricated using the vacuum infusion process. This technique was selected because it enables effective resin impregnation of the fiber network and allows better control of void formation compared to conventional hand lay-up methods. Proper resin distribution is essential for obtaining a relatively uniform composite structure and stable mechanical performance.

The materials used in this study were a commercial epoxy resin system and natural abaca fibers. Abaca was chosen due to its relatively high tensile strength and moisture resistance among plant fibers. The fibers were sourced from the Philippines, a major producer of abaca. To improve interfacial bonding between the fibers and the epoxy matrix, the fibers were treated in a 6% NaOH solution at 24 °C for 10 hours. Alkali treatment removes hemicellulose and surface impurities and increases surface roughness, which promotes mechanical interlocking with the matrix. After treatment, the fiber diameters were in the range of 150–260 μm.

The epoxy matrix had a viscosity of 500–900 mPa·s at 25 °C, a density of 1.2 g/cm^3, an equivalent molecular weight of 180 g/mol, and an epoxy index of 0.51 mol/1000 g. The curing agent was a cycloaliphatic polyamine with a density of 930–960 g/cm^3, a viscosity of 7–11 mPa·s at 25 °C, and a hydrogen equivalent weight of 48 g. The resin and hardener were mixed in a 10:1 ratio by weight. The selected resin system allows processing at room temperature without specialized equipment and provides mechanical properties typical of structural polymer systems. Its availability and moderate cost made it suitable for laboratory-scale experimental work.

2.1 Sample fabrication and preparation

Composite laminates were produced using silicone molds coated with a commercial release agent in order to prevent adhesion between the cured resin and the mold surface. Prior to infusion, the abaca fibers were manually cut to the required length and arranged inside the molds according to the intended reinforcement configuration. Particular care was taken to avoid fiber overlap and local clustering, since uneven distribution can lead to localized resin-rich or fiber-rich regions that influence mechanical and surface performance.

The epoxy resin and hardener were mixed in a 10:1 weight ratio in a clean container and stirred manually until a uniform mixture was obtained. The mixing process was carried out slowly to reduce air entrapment. Any visible air bubbles were allowed to rise to the surface before infusion. Minimizing void formation at this stage was important, as trapped air may remain within the composite structure and affect interfacial bonding and surface integrity.

The prepared fiber preforms were then infused under vacuum at a pressure of 100 mbar using a pump with a nominal capacity of 55 L/min. Vacuum infusion was selected because it allows more consistent resin penetration through the fiber network compared to conventional hand lay-up techniques. During infusion, the resin flow was visually monitored to ensure complete wetting of the fibers. If irregular flow patterns were observed, slight adjustments were made to maintain uniform impregnation.

After infusion, the laminates were left to cure at room temperature for initial hardening. To complete the polymerization process and stabilize the matrix structure, post-curing was carried out in a temperature-controlled oven. The heating schedule followed the resin manufacturer's recommendations to avoid thermal stresses or incomplete curing.

Once fully cured, the composite panels were removed from the molds and trimmed. Water jet cutting was used to obtain test specimens in order to avoid thermal damage that can occur with conventional cutting tools. This method also minimized mechanical stresses at the specimen edges.

The final sample preparation involved three steps. First, the panels were cut into rectangular specimens measuring 15 × 10 × 6.35 mm using a CNC saw to ensure dimensional consistency. Second, the contact surfaces were polished using wet abrasive papers with progressively finer grit sizes of 600, 1200, 2000, and 3000. The polishing procedure was performed carefully to avoid introducing additional surface defects while achieving a uniform finish suitable for tribological testing.

Finally, surface roughness measurements were performed using an Insize ISR-C002 roughness tester with a resolution of 0.001 μm and a maximum measurement range of 160 μm. Multiple measurements were taken along different directions of each specimen surface to verify repeatability. The measured values corresponded to the N5 surface quality standard, confirming that the prepared surfaces were appropriate for subsequent sliding tests.

2.2 Tribological Testing

Tribological measurements were carried out using a CSM nanotribometer operating in a ball-on-plate configuration with a rotational module. The experimental parameters were selected to evaluate the surface response of the composites under controlled low-load conditions. In order to allow direct comparison between specimens with different fiber contents, all tests were performed under identical contact conditions.

The contact radius was set to 2 mm, the normal load to 300 mN, and the sliding speed to 10 mm/s. Each test consisted of 500 sliding cycles. The experiments were conducted under dry conditions at room temperature, without the use of lubrication. Prior to testing, the specimens were cleaned to remove loose particles and surface contaminants.

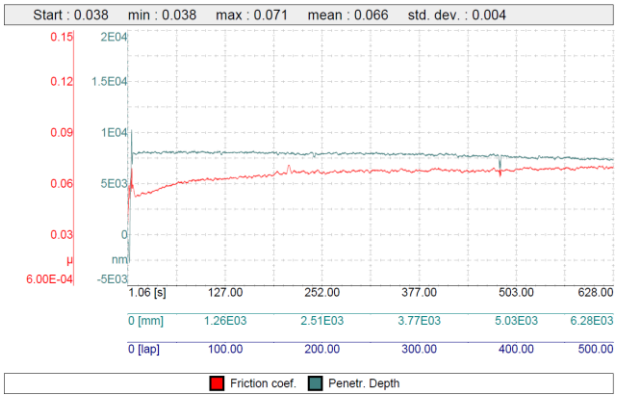
The counter body was a 100Cr6 steel ball with a diameter of 1.5 mm. This material was selected due to its high hardness and widespread use in tribological testing. After each experiment, the ball surface was inspected using optical microscopy. To minimize the influence of possible material transfer from previous tests, the ball was rotated before the next measurement so that a new contact area was engaged.

No visible damage or measurable wear was detected on the steel ball under the applied test conditions. This is consistent with the significant hardness difference between the steel counter body and the polymer-based composite samples. As a result, wear and surface modification occurred predominantly on the composite specimens, allowing the influence of fiber content and microstructural features on friction and penetration behaviour to be evaluated without interference from counter body degradation.

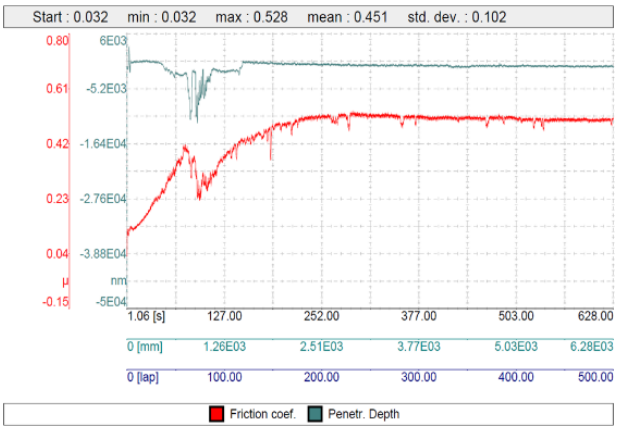
To improve repeatability, multiple tests were conducted for each fiber content, and the obtained values of friction coefficient and penetration depth were averaged. Variations observed during sliding were recorded and later correlated with the microstructural features identified through optical microscopy.

3. RESULTS AND DISCUSSION

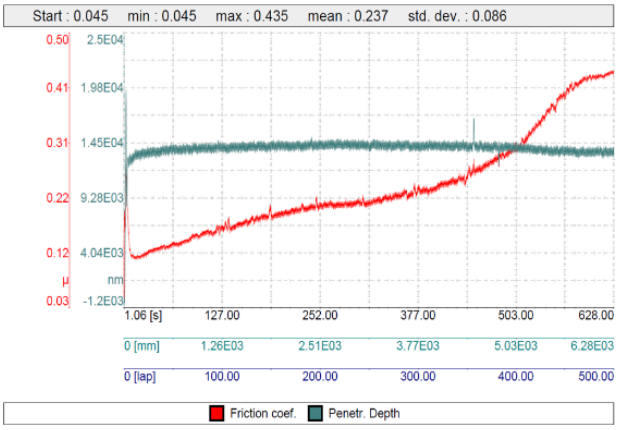
The tribological response of the investigated composites varied with fiber content under identical sliding conditions. Differences were observed in both the stability of the friction coefficient and the evolution of penetration depth during testing. The corresponding curves for specimens containing 10%, 20%, and 30% abaca fibers are presented in Figure 1.



(a)



(b)



(c)

Fig. 1. Dependence of the coefficient of friction and penetration depth of the ball on the abaca fiber content in the composite: (a) 10%, (b) 20%, and (c) 30%.

For the composite containing 10% fibers, the friction behaviour was relatively stable, and the penetration depth remained comparatively low throughout the test. The friction curve showed moderate oscillations, which are typical for polymer-based materials under dry sliding. Examination of the wear track indicated that contact occurred predominantly within matrix-rich regions, with limited exposure of reinforcing fibers at the surface. Structural imperfections were present but did not appear to significantly disturb the sliding process at this fiber fraction.

Increasing the fiber content to 20% resulted in more pronounced fluctuations in both friction coefficient and penetration depth. These oscillations can be associated with localized heterogeneities in the composite structure, including voids and variations in fiber distribution. As the contact progressed over regions with differing stiffness and interfacial bonding quality, small variations in resistance to sliding were recorded. This behaviour is mainly caused by microstructural irregularities rather than by the increase in fiber content itself.

In the case of the 30% fiber composite, the friction coefficient tended to increase gradually during the test and did not reach a clear steady-state condition within 500 cycles. The penetration depth exhibited higher variability compared to the lower fiber fractions. Although continuous and direct interaction between the ball and the fibers was not consistently observed, the higher density of structural imperfections, particularly voids and interfacial discontinuities, influenced the wear behaviour. Localized surface deformation and material removal were more irregular, indicating a less stable contact regime.

In the 30% composite, friction did not reach a steady state within 500 cycles, probably because the test duration was too short. Extending the number of cycles or increasing the applied load would likely promote more frequent fiber exposure and could alter the dominant wear mechanism. Under the present low-load conditions, matrix deformation and defect-assisted material removal appear to govern the tribological response.

The spatial distribution and orientation of fibers near the surface are not uniform. Even with rotational motion during testing, the exact location at which the counter body encounters fibers cannot be predicted. Consequently, local variations in contact geometry and stiffness may contribute to scatter in the measured friction and penetration values.

Under the applied low-load conditions, friction behaviour was primarily controlled by defect distribution within the surface layer. The quality of impregnation and the presence of voids appear to be critical factors influencing friction stability and wear behaviour in abaca fiber-reinforced epoxy composites.

As shown in Figure 2, the measured wear track widths differed noticeably between the investigated compositions. The composite containing 10% abaca fibers exhibited the smallest average wear track width, indicating more limited surface damage under the applied sliding conditions. This behaviour is consistent with the relatively homogeneous matrix structure observed for this fiber fraction.

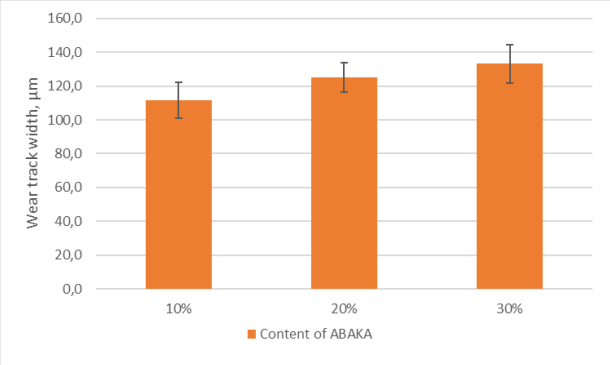


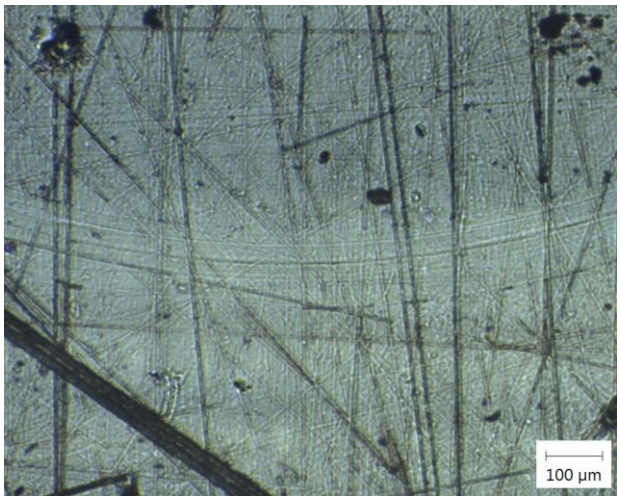
Fig. 2. Histogram of wear track widths for composites with different abaca fiber contents.

As the fiber content increased, the average wear track width also increased. Microscopic examination revealed a higher concentration of structural imperfections within the surface layer, primarily in the form of voids and air bubbles. These imperfections became more frequent with increasing fiber fraction, which likely contributed to localized stress concentrations and facilitated material removal during sliding.

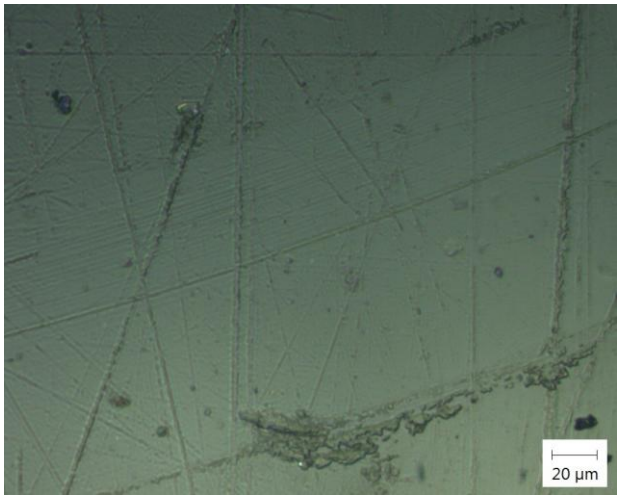
The correlation between wear track width and defect density shows that surface integrity, rather than fiber reinforcement alone, dominated the wear behaviour under these test conditions.
Optical microscopy of the composite containing 10% abaca fibers (Figure 3) revealed a relatively smooth and continuous wear track, with a limited number of visible structural imperfections both within and around the contact path. The surface morphology shows that material removal was predominantly confined to the epoxy matrix, with no significant evidence of fiber pull-out or extensive interfacial damage. Only a small amount of wear debris was detected along the outer edge of the track, indicating comparatively stable sliding conditions.

In order to assess how increasing fiber content affects surface damage mechanisms, the wear track of the composite with 20% abaca fibers was examined under the same magnification levels.

For the composite with 20% abaca fiber content, optical analysis revealed a noticeably higher concentration of structural imperfections compared to the 10% specimen. These imperfections were present both within the wear track and in the adjacent surface regions, and were larger in size as well as more numerous. The defect highlighted in Fig. 4a illustrates a void located directly within the contact path, which likely acted as a local stress concentrator during sliding.

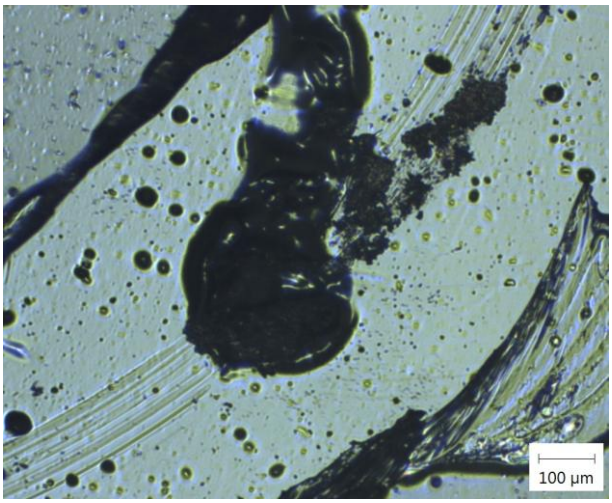


(a)

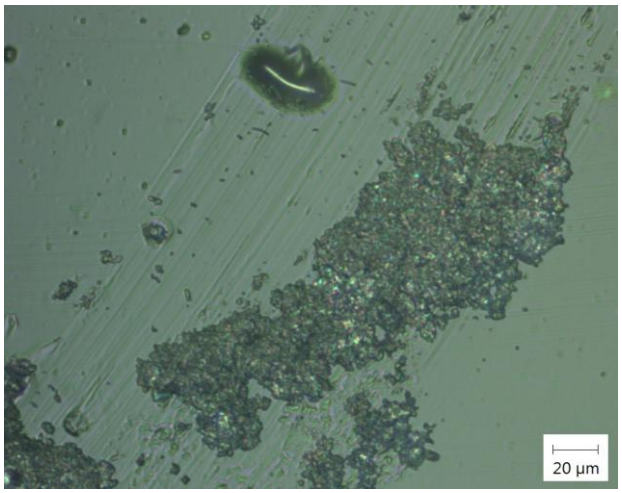


(b)

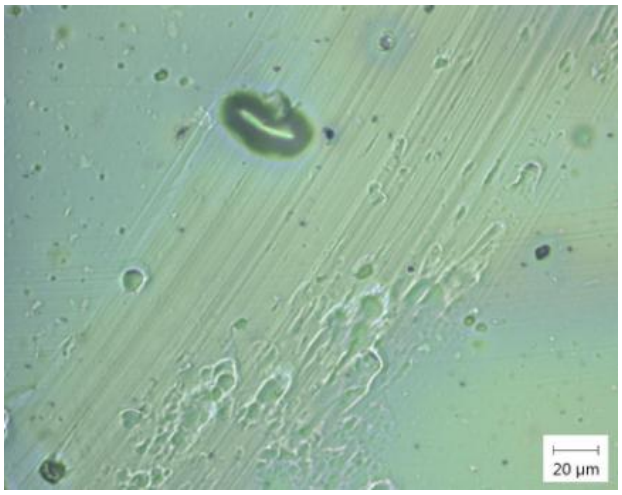
Fig. 3. Optical micrographs of the wear track for the composite containing 10% abaca fibers: (a) 5× magnification and (b) 20× magnification.



(a)



(b)

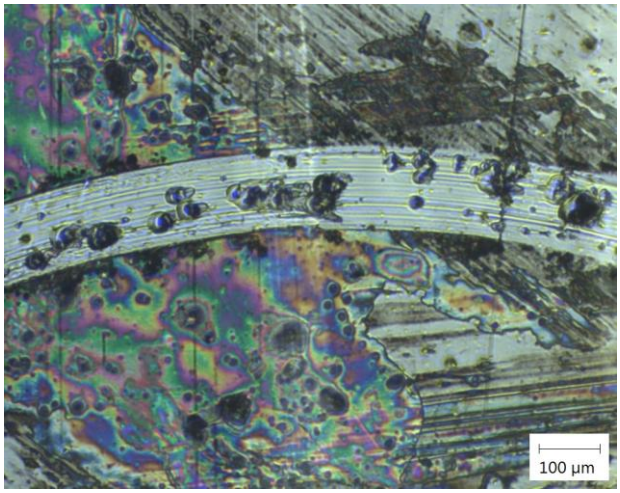


(c)

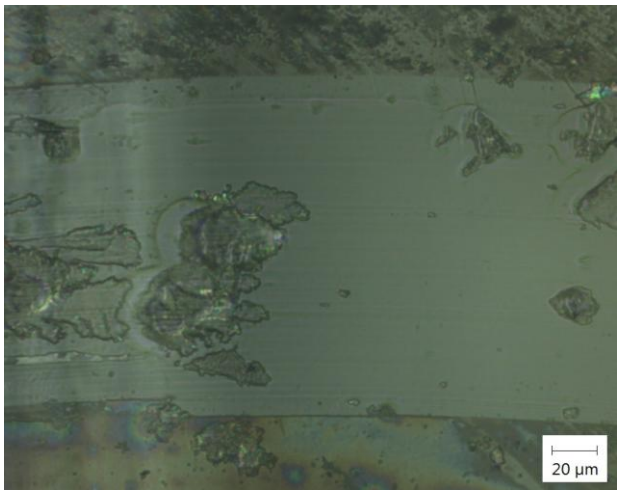
Fig. 4. Optical micrographs of the wear track for the composite containing 20% abaca fibers: (a) 5× magnification showing a structural imperfection within the track, (b) 20× magnification illustrating wear debris at the track edge, and (c) surface after gentle mechanical cleaning revealing residual surface deformation.

At higher magnification (Fig. 4b), wear debris was observed not only along the track edges but also within the contact zone. While debris commonly accumulates at the periphery of the wear track, its presence inside the track suggests intermittent detachment of material associated with surface irregularities. The debris was loosely attached, as demonstrated in Fig. 4c, where gentle mechanical cleaning removed most particles without the use of solvents. The underlying surface exhibited localized plastic deformation, indicating that the counter body had passed over detached particles, producing indentations and secondary surface damage.

With further increase in fiber content to 30%, the surface morphology changed noticeably, as illustrated in Fig. 5. A higher density of structural imperfections can be observed both within the wear track and in the surrounding regions. The wear path appears less uniform compared to the 10% and 20% composites, indicating greater variability in local contact conditions.



(a)



(b)

Fig. 5. Optical micrographs of the wear track for the composite containing 30% abaca fibers: (a) 5× magnification and (b) 20× magnification.

At higher magnification (Fig. 5b), larger voids and interfacial discontinuities are visible within the contact zone. Although continuous fiber pull-out was not clearly detected, the presence of these imperfections suggests that material removal was influenced by localized structural weaknesses rather than direct fiber fracture. This observation is consistent with the increased friction fluctuations and penetration variability recorded for this composition.

4. CONCLUSION

The results of this study demonstrate that fiber content alone does not determine the tribological performance of abaca fiber-reinforced epoxy composites under low-load sliding conditions. Instead, surface integrity and the presence of processing-induced imperfections play a dominant role in controlling friction behaviour and penetration depth at the microscale.

The composite containing 10% abaca fibers exhibited the most stable friction response and the smallest wear track width, which can be associated with a relatively homogeneous matrix structure and lower defect density. Increasing the fiber content to 20% and 30% led to greater variability in friction and penetration measurements, primarily due to a higher concentration of voids and interfacial discontinuities within the surface layer. Under the applied test parameters, matrix-dominated wear and defect-assisted material removal were more influential than direct fiber fracture or pull-out.

The absence of a clear steady-state friction regime in the 30% composite indicates that extended sliding distances or higher loads may alter the dominant wear mechanisms and promote more direct fiber participation in the contact process. Further investigations under varied loading conditions would therefore provide additional insight into the interaction between reinforcement content, microstructural quality, and tribological response.

The study confirms that careful control of fiber distribution and defect formation during processing is essential for achieving consistent tribological performance in natural fiber-reinforced epoxy composites.

REFERENCES

[1] K. Holmberg and A. Erdemir, "Influence of tribology on global energy consumption, costs and emissions," *Friction*, vol. 5, no. 3, pp. 263–284, Sep. 2017, doi: 10.1007/s40544-017-0183-5.

[2] C. Nägeli, C. Camarasa, M. Jakob, G. Catenazzi, and Y. Ostermeyer, "Synthetic building stocks as a way to assess the energy demand and greenhouse gas emissions of national building stocks," *Energy and Buildings*, vol. 173, pp. 443–460, Jun. 2018, doi: 10.1016/j.enbuild.2018.05.055.

[3] S. M. R. Dente, C. Aoki-Suzuki, D. Tanaka, and S. Hashimoto, "Revealing the life cycle greenhouse gas emissions of materials: The Japanese case," *Resources Conservation and Recycling*, vol. 133, pp. 395–403, Dec. 2017, doi: 10.1016/j.resconrec.2017.12.011.

[4] S. Shahinur and M. Hasan, "Natural Fiber and Synthetic fiber composites: Comparison of properties, performance, cost and environmental benefits," in *Elsevier eBooks*, 2019, pp. 794–802. doi: 10.1016/b978-0-12-803581-8.10994-4.

[5] M. Milosevic, P. Valášek, and A. Ruggiero, "Tribology of Natural Fibers Composite Materials: An Overview," *Lubricants*, vol. 8, no. 4, p. 42, Apr. 2020, doi: 10.3390/lubricants8040042.

[6] D. Mahesh, K. R. Kowshigha, N. V. Raju, and P. K. Aggarwal, "Characterization of banana fiber-reinforced polypropylene composites," *Journal of the Indian Academy of Wood Science*, vol. 17, no. 1, pp. 1–8, Dec. 2019, doi: 10.1007/s13196-019-00244-x.

[7] G. Rajeshkumar *et al.*, "Influence of Sodium Hydroxide (NaOH) Treatment on Mechanical Properties and Morphological Behaviour of Phoenix sp. Fiber/Epoxy Composites," *Journal of Polymers and the Environment*, vol. 29, no. 3, pp. 765–774, Oct. 2020, doi: 10.1007/s10924-020-01921-6.

[8] D. Buslovich, S. Panin, J. Luo, K. Pogosyan, V. Alexenko, and L. Kornienko, "Influence of the matrix material and tribological contact type on the antifriction properties of hybrid reinforced Polyimide-Based nano- and microcomposites," *Polymers*, vol. 15, no. 15, p. 3266, Jul. 2023, doi: 10.3390/polym15153266.

[9] M. M. Ibrahim, N. S. M. El-Tayeb, M. Shazly, and M. M. E.-S. Seleman, "An experimental study on the effect of graphite microparticles on the mechanical and tribological properties of epoxy matrix composites," *Functional Composite Materials*, vol. 5, no. 1, Feb. 2024, doi: 10.1186/s42252-023-00046-y.

[10] S. Veličković, S. Miladinović, B. Stojanović, R. R. Nikolić, B. Hadzima, and D. Arsić, "Influence of load and reinforcement content on selected tribological properties of Al/SiC/Gr hybrid composites," *Production Engineering Archives*, vol. 18, no. 18, pp. 18–23, Mar. 2018, doi: 10.30657/pea.2018.18.03.

[11] M. Milosevic, D. Dzunic, P. Valasek, S. Mitrovic, and A. Ruggiero, "Effect of Fiber Orientation on the Tribological Performance of Abaca-Reinforced Epoxy Composite under Dry Contact Conditions," *Journal of Composites Science*, vol. 6, no. 7, p. 204, Jul. 2022, doi: 10.3390/jcs6070204.

[12] L. Wenbin, H. Jianfeng, F. Jie, L. Zhenhai, C. Liyun, and Y. Chunyan, "Study on tribological properties as a function of operating conditions for carbon fabric wet clutch," *Tribology International*, vol. 94, pp. 428–436, Oct. 2015, doi: 10.1016/j.triboint.2015.10.015.

[13] Y. Liu, Y. Ma, J. Yu, J. Zhuang, S. Wu, and J. Tong, "Development and characterization of alkali treated abaca fiber reinforced friction composites," *Composite Interfaces*, vol. 26, no. 1, pp. 67–82, May 2018, doi: 10.1080/09276440.2018.1472456.

[14] V. Chaudhary, P. K. Bajpai, and S. Maheshwari, "An Investigation on Wear and Dynamic Mechanical behavior of Jute/Hemp/Flax Reinforced Composites and Its Hybrids for Tribological Applications," *Fibers and Polymers*, vol. 19, no. 2, pp. 403–415, Feb. 2018, doi: 10.1007/s12221-018-7759-6.

[15] C. W. Chin and B. F. Yousif, "Potential of kenaf fibres as reinforcement for tribological applications," *Wear*, vol. 267, no. 9–10, pp. 1550–1557, Jun. 2009, doi: 10.1016/j.wear.2009.06.002.

[16] B. F. Yousif and C. W. Chin, "Epoxy composite based on kenaf fibers for tribological applications under wet contact conditions," *Surface Review and Letters*, vol. 19, no. 05, p. 1250050, Sep. 2012, doi: 10.1142/s0218625x12500503.

[17] F. Z. Alshammari, K. H. Saleh, B. F. Yousif, A. Alajmi, A. Shalwan, and J. G. Alotaibi, "The influence of fibre orientation on tribological performance of jute fibre reinforced epoxy composites considering different mat orientations," *Tribology in Industry*, vol. 40, no. 3, pp. 335–348, Sep. 2018, doi: 10.24874/ti.2018.40.03.01.